Shashlik Calorimeter Prototypes for a Linear Collider

CALEIDO Collaboration
A.C. Benvenuti[1] , I. Britvich[6], T. Camporesi[2], P. Checchia[5], A Feniouk[6], V. Hedberg[3], V. Lishin[6], M. Margoni[5], M. Mazzucato[5], V. Obraztsov[6], M. Paganoni[4], V. Poliakov[6], F. Simonetto[5], F. Terranova[4], E. Vlasov[6]
[1]Bologna,[2]CERN,[3]Lund, [4]Milan, [5]Padua,[6]Serpukov
Presented by: M. Margoni
Dipartimento di Fisica, Università di Padova and INFN, Padua, Italy

Abstract

Two techniques for longitudinal segmentation of shashlik calorimeters are proposed. Results concerning energy resolution, impact point reconstruction and e/π separation are reported.

I. INTRODUCTION

The possibility to develop calorimeters with segmented read-out was studied in the past and different approaches were considered [1], [2]. In recent years the "shashlik" technology has been extensively studied to assess its performance at e^+e^-, ep and pp accelerator experiments [3]-[6]. Shashlik calorimeters are sampling calorimeters in which scintillation light is read-out via wavelength shifting (WLS) fibers running perpendicularly to the converter/absorber plates [7, 8]. This technique offers the combination of an easy assembly, good hermeticity and and a cheap solution compared to crystals or cryogenic liquid calorimeters.

Shashlik calorimeters are, in particular, considered to be good candidates for barrel electromagnetic calorimetry at future linear e^+e^- colliders [9]. In this context, the physics requirements impose $\sigma(E)/E \lesssim 0.1/\sqrt{E(GeV)} + 0.01$, at least three longitudinal samplings, transversal segmentation of the order of $0.9^o \times 0.9^o$ ($\sim 3 \times 3$ cm^2) and the possibility of performing the read-out in a 3 T magnetic field. The present shashlik technology can satisfy these requirements, except for the optimization of longitudinal segmentation which still needs development. The CALEIDO collaboration preposes two solutions:

- vacuum photodiodes inserted between adjacent towers in the front part of the calorimeter (CALEIDO1);

- two types of scintillator with different decay times inserted, respectively, in first and in the second longitudinal part of the calorimeter (CALEIDO2).

II. CALEIDO1

A. The prototype detector

In 1998, a prototype detector [10] was exposed to a beam with the aim of measuring the sampling capability and demonstrating that the insertion of diodes neither deteriorates critically the energy response nor produces significant cracks in the tower structure. The prototype had 25 Pb/scintillator towers, assembled in a 5×5 matrix. Each tower consisted of 140 layers of 1 mm thick lead and 1 mm thick scintillator tiles, resulting in a total depth of $25X_0$. The sampling was the finest ever used with the shashlik technique. The transversal dimension of each tower was 5×5 cm^2. In the first $8X_0$ the tiles had a smaller transverse dimension to provide room for the housing of the diodes. Plastic scintillator consisting of polystyrene doped with 1.5% paraterphenyl and 0.05% POPOP was used. Optical insulation between the towers was provided by white Tyvek paper.

The blue light produced in the scintillator was carried to the photodetector at the back of the calorimeter by means of plastic optical fibers doped with green WLS. The 1 mm diameter fibers crossed the tiles in holes drilled in the lead and scintillator plates and they were uniformly distributed with a density of 1 fiber/cm^2. The light transmission between the plastic scintillator and the fibers was in air. All the fibers from the same tower were bundled together at the back and connected to photodetectors. Two types of fibers were tested: Bicron BCF20 fibers and Kuraray Y11. In both cases, the emission peak was at about 500 nm. Light collection was increased by aluminizing the fiber end opposite to the photodetector by sputtering.

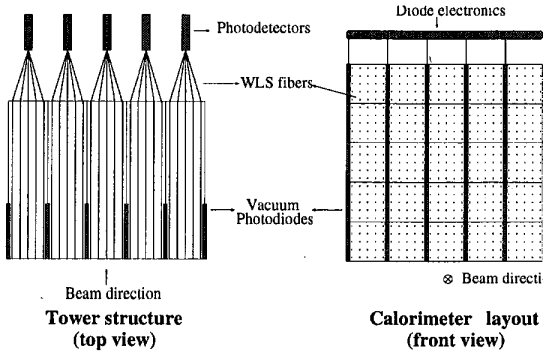

Figure 1: Layout of the calorimeter prototype (not in scale).

The light from the fibers was viewed after a 5 mm air gap by 1" Hamamatsu R2149-03 phototetrodes. Each tetrode was placed inside an aluminium housing, containing a charge sensitive JFET preamplifier and a high voltage divider. The differential output signals were shaped with a shaping time of 1.500 μs and digitized. Four towers were read-out with Hamamatsu Avalanche Photodiodes instead of tetrodes. A plexiglass light guide was used to match the smaller APD sensitive area to the fiber bundle. Preamplifiers and voltage dividers were housed in the same mechanical structure as the tetrodes.

0018-9499/00$10.00

Two types of vacuum photodiodes, viewed with a bialcali photocathode, were produced by EMI [1] (Hamamatsu [2]) with a rectangular (squared) front surface of 9×5 cm^2 (5×5 cm^2) and a thickness of 5 mm. The diodes were installed in the first part of the towers in order to sample the energy deposited in the first 8 X_0. They were in optical contact with the lateral side of the scintillator tiles and the light emitted in first part of the detector was therefore read-out twice since the photons crossing the lateral scintillator surface were collected by the diode while those reaching the fibers, either directly or after reflections, were seen by the tetrodes. Due to the direct coupling, the light collection efficiency of the diodes was much larger than that of the tetrodes/APD's and this compensated for the absence of gain in the diodes.

Most of the cells were equipped with EMI vacuum photodiodes. One diode prototype from Hamamatsu, sampling only 4 X_0, was successfully tested during the last part of the data taking. Technical characteristics of these devices are listed in table 1. The Hamamatsu prototype dimensions are such that it is possible to house two diodes in the same tower in order to obtain three longitudinal samplings. For all diodes, the same front-end electronics and read-out chain as for the tetrodes were used. The read-out electronics was positioned above the tower stacks (cfr. fig.1).

Table 1
Technical characteristics of vacuum photodiodes.

	EMI	Hamamatsu
Sensitive area	28.9 cm^2	10.9 cm^2
Diode thickness	5.0 mm	5.1 mm
Working bias	-10 V	-20 V
Capacitance	250 pF	17 pF
Energy equivalent e.noise	$\sim$ 1200 MeV	$\sim$ 900 MeV

The prototype was tested at the X5 beam in the CERN West Area. Electrons ranging from 5 to 75 GeV and pions of 20, 30 and 50 GeV were used. In order to avoid particles from channeling through fibers or diodes, the calorimeter was tilted by 3 degrees in the horizontal plane with respect to the beam direction.

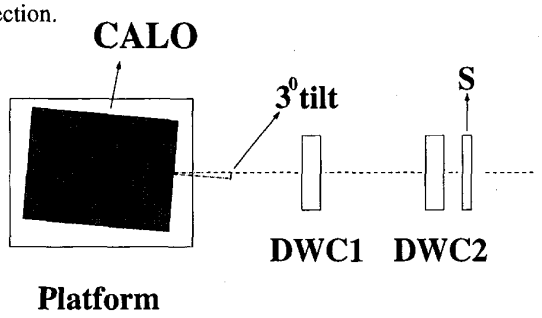

Figure 2: Top view of the testbeam setup (not in scale). "CALO" is the calorimeter tilted by 3 degrees with respect to the beam direction, "DWC1"-"DWC2" are the Delay Wire Chambers and "S" the scintillator telescope.

[1]EMI vacuum photodiode prototype D437.

[2]Hamamatsu vacuum photodiode prototype SPTXC0046.

B. *Energy resolution*

The energy response is expected to depend on the impact point since the nearer the fiber the higher the light collection efficiency. The high fiber density was used in order to reduce the non uniformity in light response to a level of a few percent. This effect was however not achieved with BCF20 fibers, due to a small scintillating component deteriorating the energy resolution. KY11 fibers, on the other hand, had a non uniformity at the level of $\pm 1.5\%$.

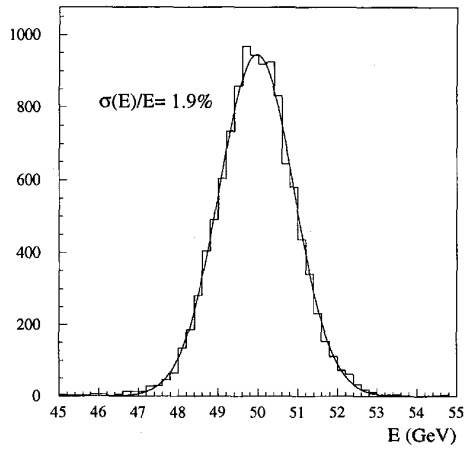

Figure 3: Energy resolution for 50 GeV electrons using tetrode read-out and KY11 optical fibers.

Fig.3 shows the energy response for 50 GeV electrons in towers equipped with Kuraray fibers and tetrode redout. The energy resolution achieved with KY11 fibers and tetrode read-out as function of the beam energy is shown in fig.4 and can be parameterized as [3]

$$\frac{\sigma(E)}{E} = \sqrt{\left(\frac{9.6\%}{\sqrt{E}} + 0.5\%\right)^2 + \left(\frac{0.130}{E}\right)^2} \qquad (1)$$

where E is expressed in GeV. The last term corresponds to the electronic noise contribution and was measured from pedestal runs.

The use of phototetrodes is not ideal for barrel calorimetry at e^+e^- colliders. Tetrodes have a rather long longitudinal dimension and must be kept at a small angle with respect to the magnetic field in order to operate with a maximum gain. The installation of Avalanche Photodiodes has been proposed by the CMS collaboration [11] as an alternative solution. Given their very good quantum efficiency ($\sim$ 80%), APD should also ensure a better energy resolution when the photoelectron statistics contribution dominates. Four APD's were installed in the prototype, as described in section A, but unfortunately no towers were equipped with APD and KY11 fibers.

[3]Alternatively, by adding the constant term in quadrature:
$\frac{\sigma(E)}{E} = \frac{10.1\%}{\sqrt{E}} \oplus 1.3\% \oplus \frac{0.130}{E}$

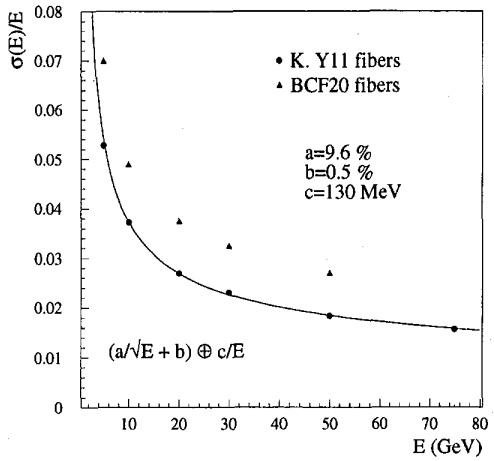

Figure 4: Relative energy resolution versus electron beam energy using tetrode read-out and KY11 optical fibers. The values obtained using the BCF20 fibers are also shown.

No significant deviations from linearity were observed up to 75 GeV which was the highest energy measured.

C. Spatial resolution

A position scan along the towers was done using 50 GeV electrons to establish the precision in the impact point reconstruction. The shower position reconstruction was based on center of gravity method corrected for the detector granularity with the algorithm suggested by [12]. The barycenter $X_b = 2\Delta \sum_i iE_i / \sum_i E_i$ (Δ is the half-width of the tower and E_i the energy deposited in tower i), was modified according to

$$X_c = b \operatorname{arcsinh}\left(\frac{X_b}{\Delta} \sinh \delta\right) \qquad (2)$$

where b is a parameter describing the transversal shower profile and $\delta \equiv \Delta/b$. Since the shower profile was not described by a single exponential, a two steps procedure was followed. The position resolution of the prototype at the cell center was 1.6 mm with 50 GeV electrons and had the following energy dependence:

$$\sigma_X(E) = \sqrt{\left(\frac{0.9}{\sqrt{E}}\right)^2 + (0.1)^2}\ \text{cm}. \qquad (3)$$

D. The diode

The EMI and the Hamamatsu diode responses to 50 GeV electrons and pions are shown in Fig. 5. The widths of both distributions were dominated by the fluctuations in the shower development. Due to the different sampling seen by the two detectors, the light signal was larger for the EMI and the fluctuations were more important in the case of the Hamamatsu prototype. On the other hand the smaller capacitance of the latter ensured a much lower electronic noise giving a comparable energy equivalent contribution as indicated in table 1.

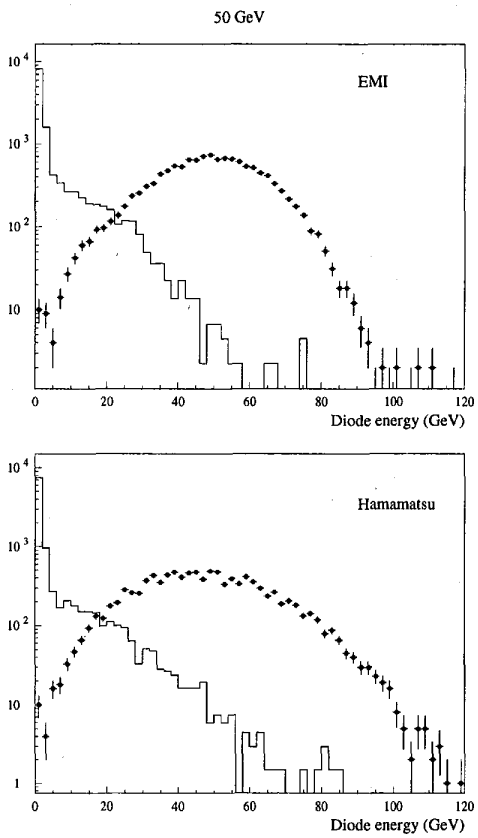

Figure 5: Energy response for 50 GeV electrons (black dots) and pions (line) for EMI and Hamamatsu diode prototypes.

Since the showers were not contained in the part of the calorimeter read-out by diodes and the longitudinal shower development depends on the energy, the response at different electron energies was not linear as shown in Fig. 6.

The dead zone between two adjacent towers due to the diode affected only a limited portion of the calorimeter and was always followed by a sufficiently long ($> 15\ X_0$) part of active detector. Therefore no complete cracks existed in the calorimeter. Nevertheless an energy loss for showers developing near the diode was visible. It was easily corrected for by using the reconstructed shower impact point. The energy response as a function of the distance y of the reconstructed position from the two tower border was parametrized as

$$E(y) = E_0 \cdot (1 - a\, e^{\frac{-y^2}{2\sigma_\pm^2}}) \qquad (4)$$

where $a = 0.075$, $\sigma_+ = 0.45$ cm for $y > 0$ and $\sigma_- = 1.19$ cm for $y < 0$. Fig.7 shows the energy response, before and after the correction, as function of the reconstructed position for 50 GeV electrons. Once the correction was introduced, the remaining non-uniformity in the energy response was due to the difference in light collection near fibers.

During 1999 test, a new diode from Hamamatsu with

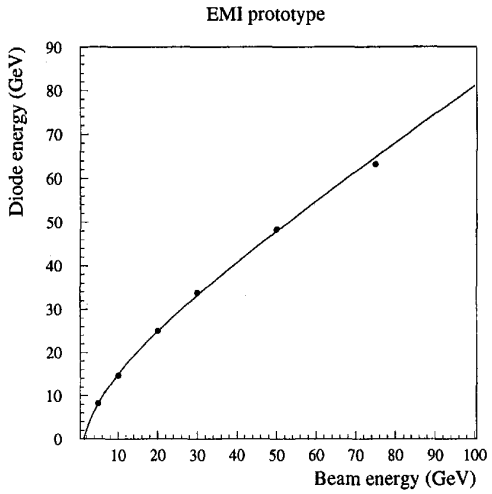

Figure 6: Energy response using the calibration coefficients computed at 50 GeV versus nominal electron beam energy (EMI diode).

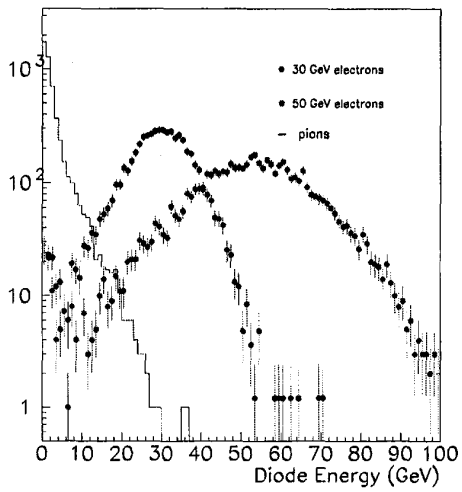

Figure 8: Energy response for 50 and 30 GeV electrons (dots) and 30 GeV pions (line) for the small Hamamatsu diode.

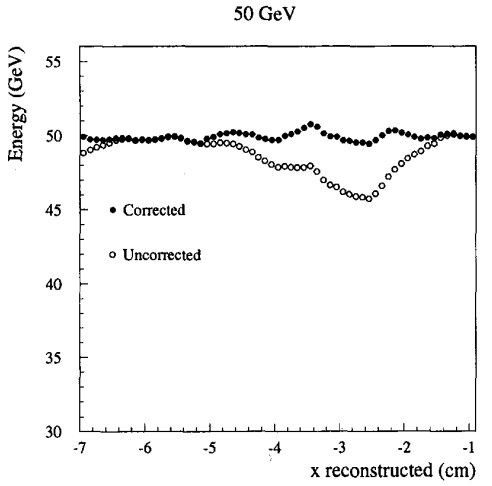

Figure 7: Energy versus reconstructed horizontal impact position before (open circles) and after (black dots) correction.

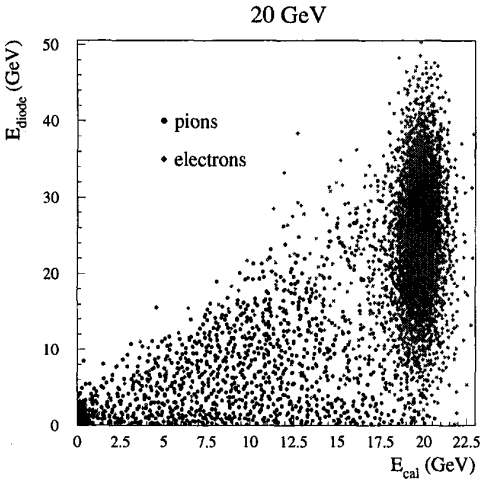

Figure 9: Diode energy versus total tetrode energy for e and π at 20 GeV.

reduced dimensions ($\sim 3 \times 5$ cm^2 lateral size to fit with towers of higer granularity) has been successfully tested. The response for pions and electrons is shown in Fig. 8.

E. e/π separation

Separation of electrons from pions was performed using discriminating variables based either on purely calorimetric data or involving also external information like the beam energy, known from the settings of main deflection magnet, which would be replaced by the momentum estimation from the tracking in a collider experiment. The fraction $\chi_E = \frac{E_{cal}}{E_{beam}}$ can be combined with pure calorimeter variables like the fraction of energy seen by the diodes and the lateral development of the shower.

Fig.9 shows E_{diode} versus E_{cal} for pions and electrons at 20 GeV. The discriminating power of the different variables in terms of pion contamination for 90% electron efficiency, at energies ranging from 20 to 50 GeV is shown in Fig.10. In most of the cases, purely calorimetric variables improve the overall separation capability with a factor ~ 2 compared with χ_E by itself. At 50 GeV the pion contamination for 90% electron efficiency is $(4.0 \pm 1.5) \times 10^{-4}$.

III. CALEIDO2

A new prototype detector was realized during spring 1999 and it has been exposed to a beam in the summer and in october. The prototype has 9 Pb/scintillator towers assembled in a 3 $\times$ 3 matrix. Each tower consists of a 29 layers of 1 mm

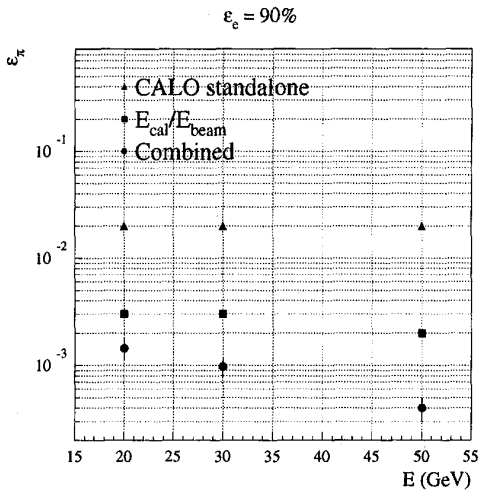

Figure 10: Pion contamination versus energy for 90% electron efficiency.

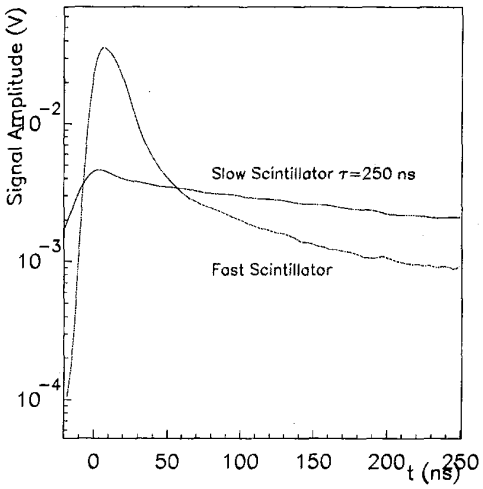

Figure 11: Signal time distribution for fast and slow scintillators

thick lead and 1 mm thick Bicron BC-444 scintillator and of 100 layers of lead and the same scintillator as the one used for CALEIDO1. The light produced by both scintillators is carried to the photodetector (FEU-84-3 photomultipliers) by means of KY11 fibers. The BC-444 scintillator has a decay time of about 250 ns and, being installed in the first $5X_0$, its signal should give the information concerning the early shower development in a time interval where the signal from the standard scintillator (which is faster than 10 ns) is much smaller. The time distribution for both scintillators is shown in Fig.11. In order to ensure a measurement without lateral leakeage in all the 9 towers, the 3 $\times$ 3 matrix was surrounded by 16 towers from CALEIDO1 prototype.

Given the short available time, only very preliminar results concerning this prototype can be presented. They are based on a quick analysis of only a fraction of the collected data. Nevertheless it can be shown that the proposed technique basically works. The signal extracted from the long component versus the total energy is shown in Fig.12 for electrons and pions. The discriminating power of the E_{slow} information (Fig.13) improves the separation capability with a factor ~ 2 compared to χ_E as described in the previous section.

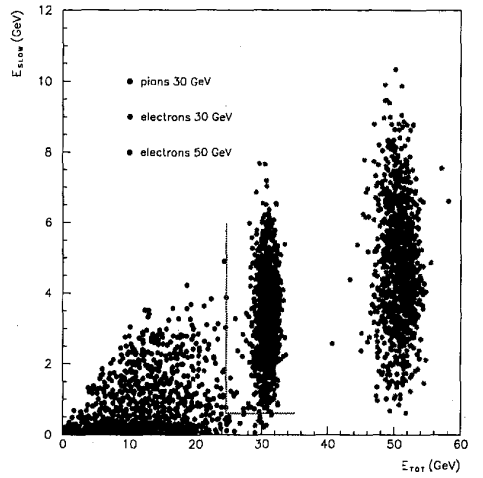

Figure 12: CALEIDO2: slow scintillator energy versus total energy for e at 30 and 50 GeV and π at 30 GeV.

IV. Conclusions

Beam test has demonstrated the technical feasibility of longitudinally segmented shashlik calorimeters in which longitudinal sampling is performed by lateral vacuum photodiodes. Due to the small dimension of the diodes and to the tilt of fibers and diodes with respect to the incoming particles, no significant cracks or dead zones are introduced. Performance in terms of energy resolution, impact point reconstruction and e/π separation seem to be adequate for applications at future e^+e^- collider experiments.

A second solution for the longitudinal segmentation based on two types of scintillator with different decay times has been tested this year. A quick analysis on a fraction of the collected data indicates the feasibility of the this technique.

V. References

[1] C. De Marzo et al., *Nucl. Instr. and Meth., A217, 1983* p. 405
[2] V. Rykalin et al., *Nucl. Instr. and Meth., A256, 1987* p. 444
[3] J. Badier et al., *Nucl. Instr. and Meth., A348, 1994* p. 74
[4] *HERA-B Design report, DESY/PRC 95-01, 1995*
[5] *LHCb Technical proposal, CERN/LHCC 98-4, 1998*
[6] S.J. Alsvaag et al., *CERN/EP 98-132, 1998*
[7] H. Fessler et al., *Nucl. Instr. and Meth. A240, 1985*, p. 284
[8] G.S. Atoyan et al., *Nucl. Instr. and Meth. A320, 1992*, p. 144
[9] R. Brinkmann, G. Materlik, J. Rossbach, A. Wagner (eds.), *DESY 1997-048, 1997*

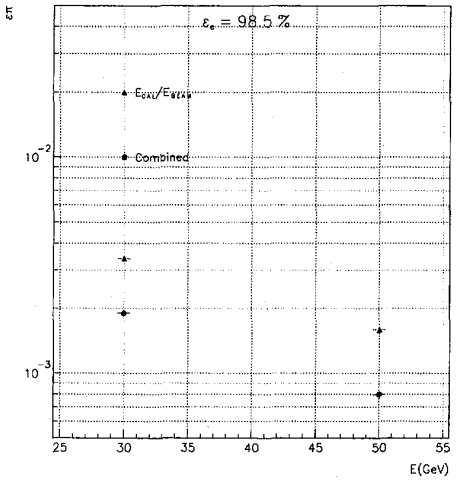

Figure 13: CALEIDO2: pion contamination versus energy for 98.5% electron efficiency.

[10] CALEIDO collab. A.C. Benvenuti et al., *CERN/EP 98-200, 1998 accepted by Nucl. Instr. and Meth. A.*

[11] *CMS Technical Proposal, CERN/LHCC 94-38, 1994*

[12] G.A. Akopdjanov et al., *Nucl. Instr. and Meth. 140, 1977* p. 441